Laser Chem., Vol. 16, pp. 207–218
Reprints available directly from the publisher
Photocopying permitted by license only

$HCl(B^1\Sigma^+)$ AND $HBr(B^1\Sigma^+)$ EMISSION FROM THE ULTRAVIOLET MULTIPHOTON DISSOCIATION OF VINYL CHLORIDE AND BROMIDE

MOHAMED OUJJA, JAVIER RUIZ, REBECA DE NALDA
and MARTA CASTILLEJO

Instituto de Química Física "Rocasolano", CSIC, Serrano 119, 28006 Madrid, Spain

(Received 17 October, 1995)

Multiphoton dissociation processes of vinyl chloride and bromide were studied with a broadband ArF laser at 193 nm and with a narrowband tunable laser in the region of 212 nm, in the peak and in the threshold of the absorption band, respectively, for both compounds. Photolysis at 193 nm gives rise to the corresponding hydrogen halide in the $B^1\Sigma^+$ excited state which results in an intense UV emission. However these emissions are absent when photodissociation was performed with the narrow band dye laser around 212 nm. These results, together with a calculation of the observed spectra, give further support to a mechanism which invokes one-photon resonant absorption of vibrationally hot ground state hydrogen halide as the process which populates the excited $B^1\Sigma^+$ state of the fragment.

KEY WORDS: Vinyl halides, multiphoton dissociation, photofragmentation.

INTRODUCTION

The vinyl chloride and bromide molecules have broad absorption bands in the UV region with a maximum of absorption around 190 nm which has been assigned to the $^1(\pi^*,\pi)$-X^1A' transition.[1] The ultraviolet dissociation of vinyl chloride and bromide has been studied by several groups. Umemoto *et al.*[2] measured the translational energy distribution of Cl and HCl fragments resulting in the photodissociation of vinyl chloride at 193 nm. The high efficiency of the HCl elimination is attributed to a rapid internal conversion from the (π^*,π) excited parent to the electronic ground state.[1,2] On the other hand Gordon *et al.*[3] have measured the rotational energy distribution of HCl ($v' = 0, 1, 2$) produced in the photodissociation of vinyl chloride at 193 nm by $2 + 1$ resonantly enhanced multiphoton ionization (REMPI) and have discussed[4,5] the mechanism of the UV photodissociation of chloroethylenes by determining the Doppler profiles, spatial anisotropy and power dependence of Cl, H and HCl fragments. Y. T. Lee *et al.*[6] have studied the UV photodissociation of vinyl bromide by measuring the translational energy distribution and anisotropy parameters of the Br and HBr products at 193 nm. This process has been also investigated theoretically[7] by using a classical trajectory method and their results are consistent with an HBr elimination mechanism which proceeds

subsequently to internal conversion of the excited parent molecule to its ground state prior to dissociation.

The work performed in the UV one photon dissociation processes of haloethylenes has produced a quite complete picture of the mechanisms involved. In contrast, the UV multiphoton processes have been less studied and appear more controversial. Rossi and Helm[8] proposed a mechanism for HCl^+ production following multiphoton dissociation of vinyl chloride at 193 nm, which proceeds via near-resonant two-photon absorption of vibrationally excited HCl originated in the one-photon dissociation of the parent. These ideas have been criticized by Gordon *et al.*[9] These authors claim that the HCl^+ fragment is produced by a three-photon resonant process in which the initial step is the production of a long-lived state of vinyl chloride which can, either dissociate to give ground state fragments, or absorb another photon to give an electronically excited HCl fragment. Regarding the production of neutral fragments Bartolomé *et al.*[10] reported the emission from $HCl(B^1\Sigma^+)$ and $HBr(B^1\Sigma^+)$ resulting from the 193 nm photodissociation of vinyl chloride and bromide respectively. A mechanism based on the one-photon-resonant absorption of vibrationally excited HCl, formed after one-photon dissociation of the parent, was proposed.

As mentioned above the photodissociation dynamics of vinyl chloride and bromide near the absorption peaks has been studied extensively. However, there have been no such experiments at threshold regions of the absorption bands, where the dynamics can differ from that of the maximum of the absorption band. The purpose of this work is to give more insight into the mechanism of excited hydrogen halide formation in the UV multiphoton dissociation of the corresponding vinyl compound by studying the process at several wavelengths, including the region of the absorption peak at 193 nm with an ArF laser and longer wavelengths in the shoulder of the absorption band, with a narrowband tunable laser around 212 nm.

EXPERIMENTAL

The experimental systems used for this work have already been described[11,12] and only a short summary will be given here. Fluorescence spectra from HCl and HBr electronically excited photofragments were recorded in the 190 to 240 nm range following photolysis of vinyl chloride and vinyl bromide at 193 nm with an ArF excimer laser and at several wavelengths around 212 nm with a narrowband frequency doubled dye laser. In both cases photolysis radiation was focused in a glass cell fitted with quartz windows containing the flowing haloethylene samples. Experiments of photodissociation at 193 nm were performed with an ArF laser typically delivering 100 mJ of energy in pulses about 15 ns wide. The laser output was focused with a 2 m focal length quartz lens in a region placed 20 cm behind the observation zone. The fluorescence at right angles to the exciting laser beam was dispersed by a 0.5 m Jarrell-Ash monochromator and viewed by a 9816 QB photomultiplier; the spectra were corrected for shot-to-shot laser fluctuations by an appropriate reference signal. Both signal and reference were sent to gated integrators and boxcar averagers (Stanford Research Systems SR250) and digitized by an A/D converter built

into a programmable unit which performs automatic scanning of the monochromator, proper timing of trigger pulses of laser and boxcar, and finally transfers the signals to a microcomputer for data storage and analysis.

In experiments of photodissociation around 212 nm the photolysis radiation was obtained by frequency doubling the output of a narowband dye laser pumped by a XeCl excimer laser. The dye laser, operating with Stilbene 3 dye, was frequency doubled in a BBO crystal delivering typically 0.3 mJ of radiation tunable from 210 to 215 nm with a bandwidth of 0.4 cm^{-1}. The laser pulse was focused at the observation region with a quartz lens of 16 cm focal length. At these photolysis wavelengths the fluorescence intensity was weak and a lower resolution high intensity Bausch and Lomb monochromator was used to record photofragment fluorescence spectra.

The fluorescence cell was connected to a glass vacuum system routinely operating at a vacuum of 10^{-5} Torr. Typical pressures of flowing compounds, measured directly in the cell with a capacitance manometer (MKS Baratron $10^{-3}-1$ Torr), ranged between 100 and 960 mTorr depending on the experiment. Vinyl chloride and bromide were purified by trap-to-trap distillation prior to use.

RESULTS

In previous work it has been reported[10,13] that photodissociation of vinyl chloride and vinyl bromide at 193 nm gives rise to a strong emission in the region of wavelengths below 240 nm originated by $HCl(B^1\Sigma^+)$ and $HBr(B^1\Sigma^+)$ photofragments respectively. In the present study we recorded both emission spectra with a resolution of 0.32 Å which is sufficient to resolve almost completely the rotational structure of the involved electronic transitions. The resulting spectra, obtained following 193 nm photolysis of 100 m Torr of the parent vinyl halide, are shown in Figures 1(a) and 2(a). As can be seen in the figures, the long wavelength limit of the spectrum is shifted from 238.0 nm in HCl to 221.5 nm in HBr, in agreement with previously reported observations.[14] The above spectra were obtained by mildly focusing the photolysis laser in the observation region. Therefore the Mulliken bands, corresponding to the $C_2(D^1\Sigma_u^+ - X^1\Sigma_g^+)$ transition, which appear around 232 nm[10] at high laser intensities, are not detectable in the present experimental conditions.

In order to understand the mechanism of production of HCl and HBr in the two-photon dissociation of vinyl chloride and bromide in the UV, photodissociation of both vinyl halides was also studied at several wavelengths around 212 nm, in the threshold region of the absorption band in both compounds. Emission spectra were recorded from 200 to 600 nm; in the 240 to 600 nm range a set of emission bands were observed corresponding exactly with the photofragment emissions detected in the 193 nm photolysis. The intensity of these bands was found four times higher in the photolysis of vinyl bromide than in the case of vinyl chloride. These emission bands, shown in Figure 3 for the case of vinyl bromide, were readily assigned to the electronically excited CH photofragment formed in the $A^2\Delta$ state and to the C_2 photofragment formed in its $d^3\Pi_g$ and $C^1\Pi_g$ excited states, ie. the

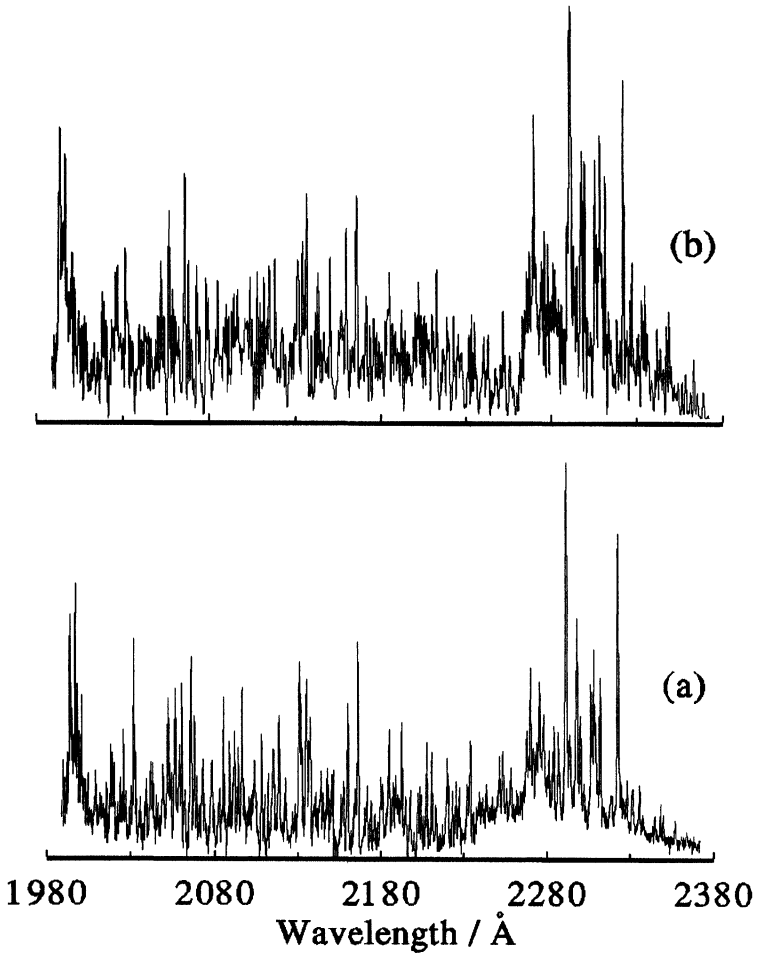

Figure 1 $HCl(B^1\Sigma^+)$ fluorescence spectrum, obtained by photodissociation of vinyl chloride at 193 nm. The resolution is 0.32 Å. (a) Experimental spectrum obtained by photolysis of 100 m Torr of vinyl chloride. The spectrum was corrected for laser power fluctuations and by the spectral response of the detection system. Each point in the spectrum is an average over five laser shots. (b) Simulated spectrum.

Swan and Deslandres-D'Azambuja bands respectively. Following the photolysis of vinyl bromide a weak emission at 232 nm corresponding to the carbon Mulliken bands was also observed. This emission was not detected in the photolysis of the chloride compound, probably due to the lower intensity of the excited C_2 fragment emissions, resulting from the photolysis of the latter.

A study of the dependence of all the observed photofragment C_2 and CH emissions with laser energy was performed. On energy grounds three photons of wavelength around 212 nm are needed to produce the photofragments $CH(A^2\Delta)$ and $C_2(C^1\Pi_g)$ and $C_2(D^1\Sigma_u^+)$ and two photons are the minimum energy required to form $C_2(d^3\Pi_g)$. A logarithmic plot of the dependence of the $C_2(D^1\Sigma_u^+)$ emission at

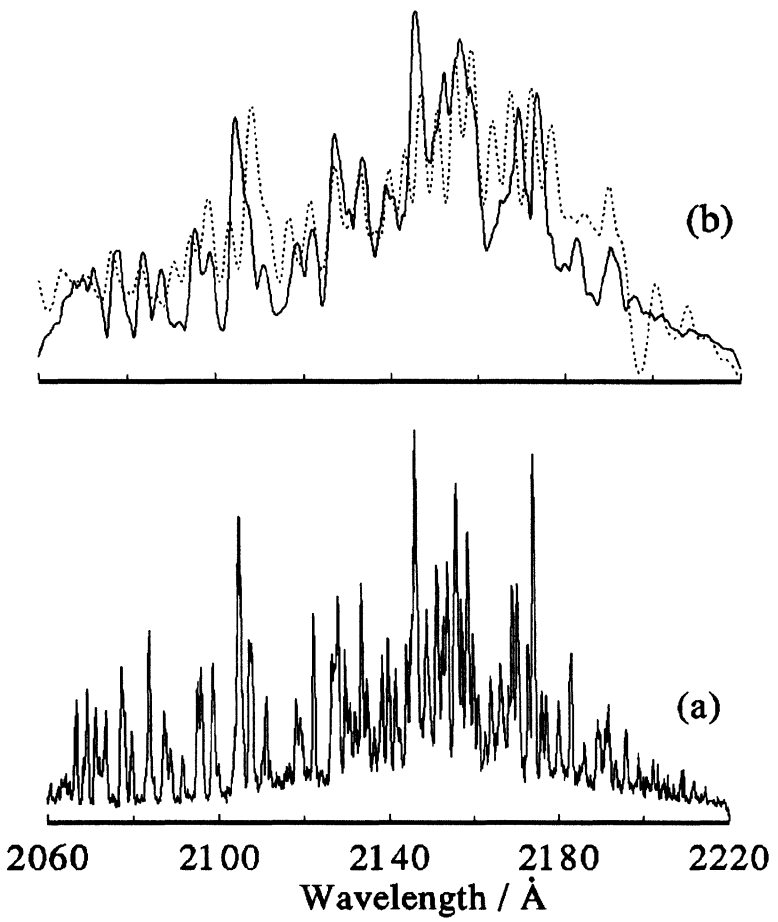

Figure 2 $HBr(B^1\Sigma^+)$ fluorescence spectrum obtained by photodissociation of vinyl bromide at 193 nm. (a) Experimental spectrum obtained by photolysis of 100 m Torr of vinyl bromide taken with a resolution of 0.32 Å. The spectrum was corrected for laser power fluctuations and by the spectral response of the detection system. Each point in the spectrum is an average over five laser shots. (b) Solid line: experimental spectrum with an apparent resolution of 3 Å and dashed line: calculated spectrum for m = 3 (see text).

232 nm on laser energy is represented in Figure 4; the straight line best fitting the plot has a slope equal to 2.0 ± 0.2. Both $CH(A^2\Delta - X^2\Pi)\,\Delta v = 0$ and $C_2(C^1\Pi_g - A^1\Pi_u)\,\Delta v = +1$ emissions measured at 431 and 360 nm respectively, exhibit also a quadratic dependence with laser energy. The $C_2(d^3\Pi_g - a^3\Pi_u)\,\Delta v = +1$ emission, measured at 470 nm, scales with a law in which the exponent is 1.6 ± 0.2. These results indicate that most probably one step of the multiphoton process is saturated.

Photolysis of vinyl chloride and bromide around 212 nm did not yield any appreciable hydrogen halide emission. A careful search of any emission that could appear in the 200 to 238.0 nm range for the case of the chloride compound and in the 200 to 221.5 nm region for the case of the bromide compound was performed by

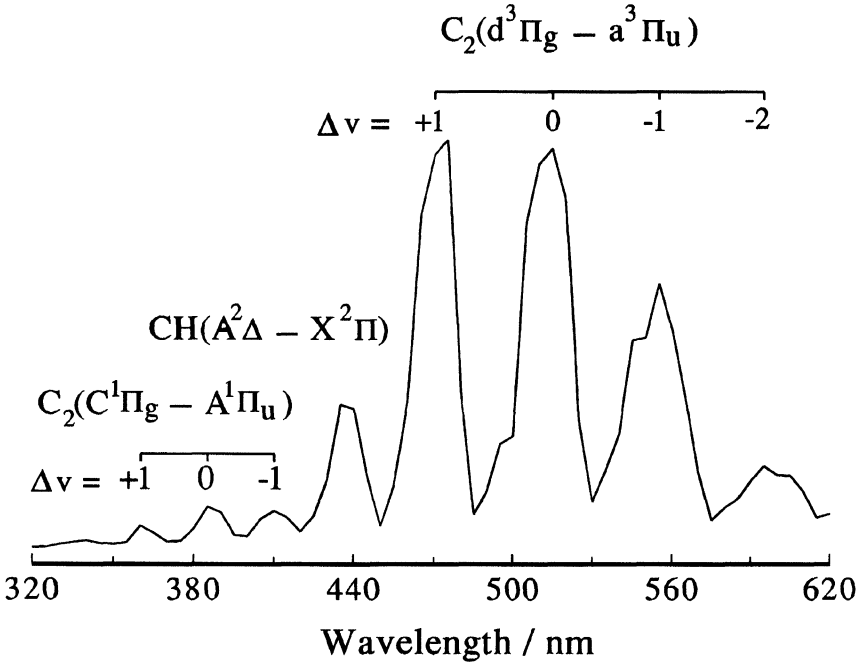

Figure 3 Photofragment emission spectrum obtained by photodissociation of 960 m Torr of vinyl bromide at 214.1 nm. The spectral resolution is 40 nm.

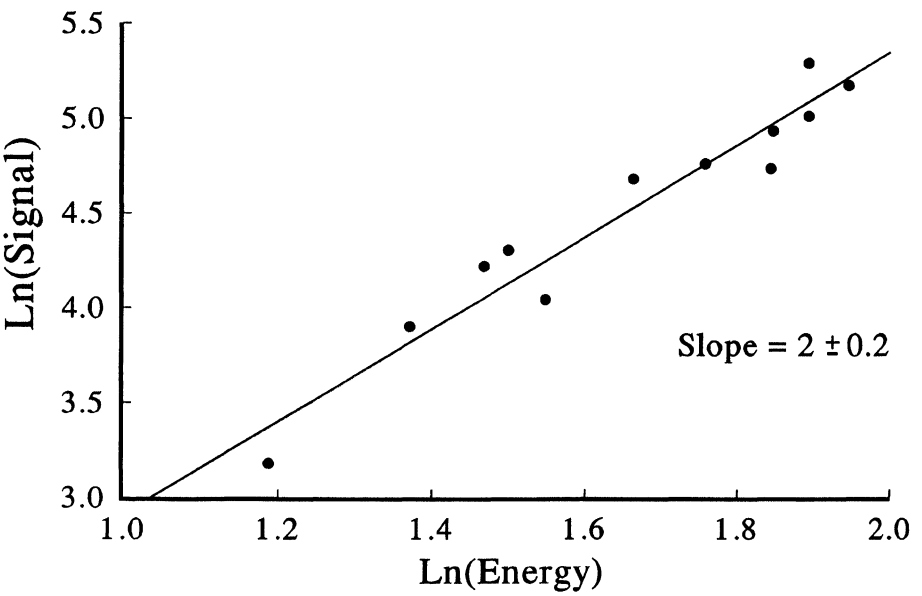

Figure 4 Logarithmic plot of the $C_2(D^1\Sigma_u^+)$ photofragment fluorescence at 232 nm as a function of laser energy obtained by photolysis of 960 m Torr of vinyl bromide. The photolysis wavelength was 214.1 nm. Data were fitted to a straight line with a slope equal to 2.0 ± 0.2.

finely tuning the laser around 212 nm in steps of 0.02 Å without resulting in a detectable emission.

To get more insight into the mechanisms which are responsible of the electronically excited hydrogen halide emission resulting from photolysis of the parent haloethylene we attempted to simulate the emission spectra of both photofragments following photolysis at 193 nm. The rovibrational population distributions which are responsible of the observed spectra, were estimated by using a computer program based on a truncated singular value decomposition method.[15] The method involves firstly the calculation of wavefunctions and transition matrix elements between the pair of electronic states involved in the emission. Secondly the resolution of a system of coupled linear equations, where the unknowns are the rovibrational population distribution of the molecular excited state, and finally the spectral simulation. The details of the simulation in each case are given below.

Simulation of the Emission Spectrum of the HCl ($B^1\Sigma^+$) Photofragment

The experimental spectrum shown in Figure 1 (a) is considered to be due to the participation of two electronic transitions: a bound-to-bound $B^1\Sigma^+ - X^1\Sigma^+$ transition, responsible of the observed structure of lines in the spectrum, and a bound-to-free $B^1\Sigma^+ - A^1\Pi$ transition, which accounts for the continuum around 228 nm on which the lines of the $B^1\Sigma^+ - X^1\Sigma^+$ transition are superimposed. All the calculations described below were performed for $H^{35}Cl$. The potential energy functions of the three states involved in the spectrum have been modelled in the range of internuclear distances between 0.65 and 6.0 Å and are depicted in Figure 5 (a). For the $X^1\Sigma^+$ state, in the range from 0.65 to 3.5 Å, we used an analytical Hamiltonian obtained by performing a fitting of the HCl spectroscopic data set.[16] Extrapolation at long internuclear distances up to 6.0 Å was done according with[17] by using a multipolar expansion of the type $V(R) = D - \Sigma_n C_n/R^n$ for $n = 6, 8, 10$; with $D = 37243\ cm^{-1}$ being the dissociation energy, and with coefficients $C_6 = 1.59\ 10^5\ cm^{-1}\ A^5$, $C_8 = 1.89\ 10^5\ cm^{-1}\ A^8$ and $C_{10} = 4.32\ 10^7\ cm^{-1}\ A^{10}$ taken from.[17] For the ion-pair state $B^1\Sigma^+$, an effective analytical potential energy function was available in the 1.4 to 3.9 Å range.[18] Extrapolation in the repulsive branch was performed with a model of the type ae^{-bR}. Again, in the long internuclear distances region, a multipolar expansion of the type indicated above was adopted. A potential energy curve for the dissociative $A^1\Pi$ state, provided by Ballint-Kurti *et al.*,[19] was used in the complete range of internuclear distances. The relative contribution to the $HCl(B^1\Sigma^+)$ emission spectrum of the $B^1\Sigma^+ - X^1\Sigma^+$ and $B^1\Sigma^+ - A^1\Pi$ transitions was taken into account by considering the dipole transition moments, calculated by van Dishoek *et al.*[20] Although the dependence of the dipole transition moments on internuclear distance was introduced in our calculations, similar results, concerning the distribution of populations and the simulated spectrum, were obtained by considering average values of 1.2 and 0.4 a.u. for the dipole transition moments of the bound-to-bound and bound-to-free transitions respectively. By using the above models of potential energy functions and electronic dipole transition moments, we have calculated transition energies, Franck-Condon overlap integrals,[21] and Hönl-London factors for the B – X and B – A transitions. Transitions between $v' = 0$–6 in

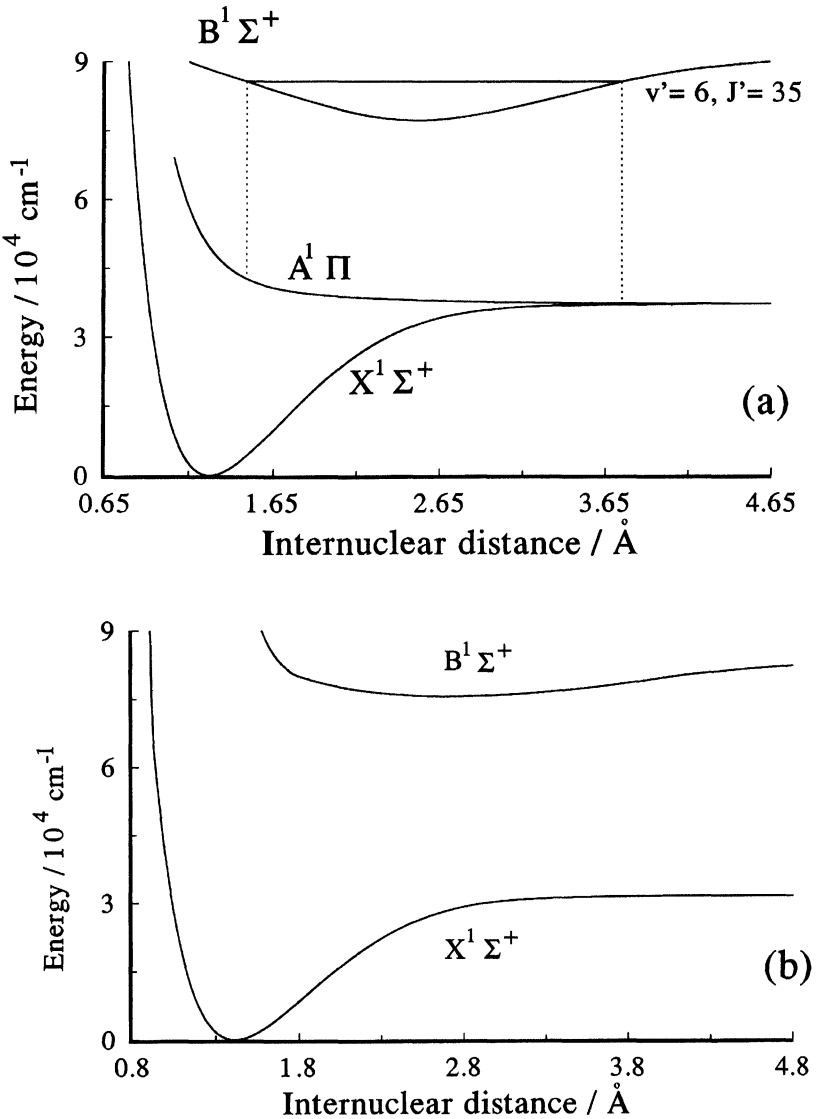

Figure 5 Potential energy functions used to simulate the emission spectrum of the: (a) $HCl(B^1\Sigma^+)$ photofragment; the classical turning points of the $B^1\Sigma^+$ $v' = 6$, $J' = 35$ state, together with the corresponding Born-Oppenheimer region in the repulsive $A^1\Pi$ are indicated. (b) $HBr(B^1\Sigma^+)$ photofragment. For details of the curves see text.

the B upper state, involving rotational levels up to $J' = 35$ and $v'' = 9-17$ in the X lower state were considered. The calculated transition energies have been compared with the observed line positions.[22] The differences are not higher than 4 cm^{-1} and represent a reasonable agreement when compared with the spectral resolution of our experimental spectrum, of around 5 cm^{-1}. In the dissociative $A^1\Pi$ state, levels with energies in the range between 37350 and 42750 cm^{-1} were considered. As indicated

in Figure 5, these energy limits are determined by the classical turning points of the $v' = 6$, $J' = 35$ upper state, which is the level with highest energy considered in our calculations. Franck-Condon overlap integrals for the bound-to-free transitions were evaluated in steps of 50 cm^{-1} in the indicated energy range. Figure 6 shows the population distribution estimated by applying the mentioned algorithm to the experimental spectrum of Figure 1. The calculated spectrum is also shown in Figure 1 and appears to be in reasonably good agreement with the experimental spectrum. The obtained rotational distributions for each vibrational levels from $v' = 0$ to 6 show groups of selected J' levels significantly populated. These results suggest the formation of $HCl(B^1\Sigma^+)$ through a selective mechanism which populates a narrow set of rovibrational levels of this state. We have calculated the set of v', J' levels which could be excited from certain v'', J'' levels of $HCl(X^1\Sigma^+)$ by resonant absorption within the laser bandwidth of a second ArF photon. By assuming that the

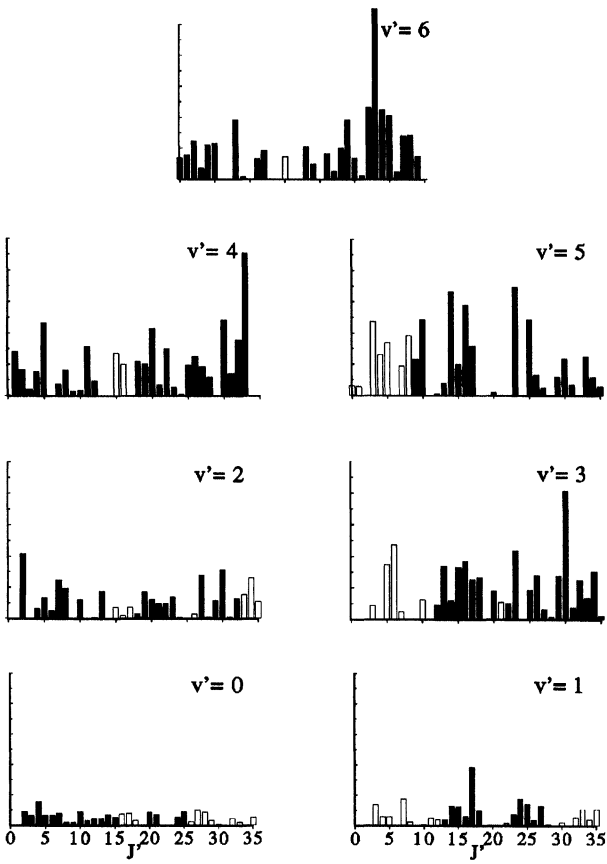

Figure 6 $HCl(B^1\Sigma^+)$ v', J' distributions which produce the simulated spectrum of Figure 1. The vertical scale is the same for all vibrational states. The solid bars indicate the set of populated $v'J'$ levels which would be promoted from the HCl ground state by resonant absorption within the ArF laser spectral profile.

spectral profile of the ArF laser covers the region between 51150 to 52000 cm^{-1} a total number of 160 $v'J'$ levels would be populated in the resonant process. The populated levels included in this set are indicated in Figure 6. Inspection of this Figure reveals that most of the levels which show an appreciable population as a result of the calculation could be promoted from the HCl ground state by resonant absorption of an ArF laser photon.

Simulation of the Emission Spectrum of the HBr($B^1\Sigma^+$) Photofragment

Due to the lack of information about the dissociative $A^1\Pi$ state we have not included it in the simulation of the emission spectrum of the HBr($B^1\Sigma^+$) photofragment, although by analogy with HCl, some contribution from the bound-to-free $B^1\Sigma^+ - A^1\Pi$ transition should be expected. Models for internuclear potentials of the ground $X^1\Sigma^+$ and excited $B^1\Sigma^+$ states have been built in the range of distances between 0.8 and 6 Å. The ground state has been represented in the 0.8 to 2.8 Å region by an analytical function given by Coxon.[23] The attractive branch up to 6 Å is represented by a multipolar expansion of the same type as the one used in the ground state of the HCl molecule. Values of the coefficients are $D = 31625$ cm^{-1},[24] $C_6 = 2.04\ 10^5$ cm^{-1} A^5, calculated according to[25] from ionization potentials and polarizabilities of the two atoms forming the molecule,[26] $C_8 = 1.76\ 10^5$ cm^{-1} A^8 and $C_{10} = 4.58\ 10^7$ cm^{-1} A,[10] calculated by imposing the condition of continuity to the potential function at $R = 2.8$ Å.

Construction of the potential energy function for the $B^1\Sigma^+$ upper state presents more difficulties as spectroscopic information on the $B^1\Sigma^+ - X^1\Sigma^+$ transition in HBr is incomplete. In absorption, a $B^1\Sigma^+ - X^1\Sigma^+(v' - v'' = 0)$ progression has been identified. The assignment of the first band is uncertain and was labelled as the $(v' = m - v'' = 0)$ band with all the subsequent members of the progression relative to it. Transition energies up to the $(v' = m + 13 - v'' = 0)$ band with J values up to 10 were reported.[27] An RKR effective potential for the $B^1\Sigma^+$ state has been built considering a set of spectroscopic constants derived from the available spectroscopic information as follows: values of ω_e and $\omega_e x_e$ were obtained by fitting the origin of the vibrational bands to a second order expansion on $(v' + 1/2)$. The resulting values are $\omega_e = 479.55$ cm^{-1} and $\omega_e x_e = 0.3$ cm^{-1}. Attempts to obtain the rotational constant B_e in the same way, by fitting the energies of rovibrational levels as a function of J, resulted in too large a value for the rotational constant. The derived equilibrium internuclear distance, related to the rotational constant by the expression $B_e = h/8\pi^2\ (100c)\,\mu\ R_e^2$, was too small compared with the value given in[14] of 2.7 Å, needed to understand the $B^1\Sigma^+ - X^1\Sigma^+$ emission spectrum. Therefore in our calculation we used $B_e = 2.3$ cm^{-1} which reproduces satisfactorily the estimated equilibrium internuclear distance of the state. The value of T_e obviously depends of the value given to m. With the above $\omega_e = 479.55$ cm^{-1}, it is possible to derive T_e by assuming a given value for m. For $m = 2$ and 3 the corresponding values of T_e are 76084 and 75604 cm^{-1}. These numbers have to be compared with the estimation of Stamper and Barrow[14] of $T_e = 75974$ cm^{-1}. Two different RKR potentials were built for the $m = 2$ and $m = 3$ cases, each one producing a different simulated spectrum to be compared with the experimental spectrum in order to find the best agreement.

With the $B^1\Sigma^+$ and $X^1\Sigma^+$ potentials described above, Franck-Condon overlap integrals and Hönl-London factors have been calculated for vibrational bands ($v' - v''$) with $v' = 0 - 7$ and $v'' = 12-17$. Rotational levels up to $J = 25$ were considered. To simulate the spectrum the energies of the transitions were taken from[27] when available. For unreported transitions, the energy was calculated with the effective spectroscopic constants indicated above. The quality of the approximations used to build an effective $B^1\Sigma^+$ state potential made it difficult to simulate the high resolution used to record the experimental spectrum. In order to compare both spectra, the latter was convoluted with a gaussian function which provided an apparent resolution of 3 Å. The best agreement between experimental and simulated spectra was obtained for $m = 3$. Figure 2(b) shows both spectra in this case. The population distributions which yields the calculated spectrum of Figure 2 are affected by relatively large errors mainly associated with the limited spectral resolution and the uncertainties in the model potentials used in the calculations. The obtained population distributions show, as in the case of HCl, that only groups of selected J′ levels in each vibrational state are significantly populated.

DISCUSSION

In a previous paper[10] a mechanism for $HCl(B^1\Sigma^+)$ formation in the ArF laser multiphoton dissociation of vinyl chloride was proposed. The mechanism proceeds in two steps: the first step leads to formation of vibrationally hot ground state HCl, in the second step resonant absorption of a second ArF laser photon by certain vibrationally excited v″, J″ levels of $HCl(X^1\Sigma^+)$ populates a relatively narrow v′J′ set in the observed $HCl(B^1\Sigma^+)$ state. The simulation of the $HCl(B^1\Sigma^+)$ emission, presented in this work, is more accurate as it includes contributions from both bound-to-bound $B^1\Sigma^+ - X^1\Sigma^+$ and bound-to-free $B^1\Sigma^+ - A^1\Pi$ transitions and uses updated model potentials. Moreover, to simulate the spectrum no constraints are imposed over the rovibrational population distribution and it is the set of populations, obtained by the method described above, which show signs of the existence of a resonant mechanism. The lack of HCl emission in the dissociation at 212 nm appears to give further support to these ideas. A process of $HCl(B^1\Sigma^+)$ formation involving a two-photon excited vinyl chloride parent molecule, similar to the one proposed by Gordon *et al.*[9] for HCl^+ formation, would not explain the differences observed in the photolysis at 193 and 212 nm. On the contrary if $HCl(B^1\Sigma^+)$ rovibrational states are populated by resonant absorption of a laser photon from vibrationally hot $HCl(X^1\Sigma^+)$, photolysis by a broad band ArF laser could populate a range of rovibrational states, whereas photolysis with a narrowband laser at 212 nm would only populate a v′J′ level if there exist a $B^1\Sigma^+ - X^1\Sigma^+$ ($v'J' - v''J''$) transition which could be resonant with the photon energy. Subsequently the possible emission from a single state would be difficult to observe if the fluorescence is dispersed with a monochromator. These arguments would explain the absence of $HCl(B^1\Sigma^+)$ emission in the photolysis at 212 nm.

Regarding vinyl bromide, the calculation of the $HBr(B^1\Sigma^+)$ spectrum following the ArF photodissociation of the parent is less accurate as compared with HCl.

Therefore the conclusions we could draw in this case are less definitive. The calculated spectrum shows a reasonable agreement with the experimental spectrum if the origin of the vibrational progression m in the $B^1\Sigma^+ - X^1\Sigma^+$ electronic transition[27] is set to 3. Nevertheless the magnitude of errors affecting the estimated population distribution precludes the possibility of performing a quantitative analysis of these distributions. The lack of HBr emission in the photolysis of vinyl bromide at 212 nm is, as in the case of vinyl chloride, a fact that supports the resonant mechanism of formation of the corresponding hydrogen halide.

Acknowledgements

This work was financed by Spanish DGICYT (PB93-0145-C02-01) and by the Human Capital and Mobility Programme of the European Community (CHRX-CT94-0485). We thank Prof. G.G. Ballint-Kurti for providing an analytical form of the $HCl(A^1\Pi)$ potential and Prof. J. A. Coxon for making available a model of the $HCl(X^1\Sigma^+)$ ground state potential. Discussions with Dr. Margarita Martín were extremely valuable in the course of this work.

References

1. M. J. Berry, *J. Chem. Phys.*, **61** 3114 (1974).
2. M. Umemoto, K. Seki, H. Shinohara, U. Nagashima, N. Nishi, M. Kinoshita and R. Shimada, *J. Chem. Phys.*, **83** 1657 (1985).
3. P. T. A. Reilly, Y. Xie and R. J. Gordon, *Chem. Phys. Lett.*, **178** 511 (1991).
4. Y. Mo, K. Tonokura, Y. Matsumi, M. Kawasaki, T. Sato, T. Arikawa, P. T. A. Reilly, Y. Xie, Y. Yand and R. J. Gordon, *J. Chem. Phys.*, **97** 4815 (1992).
5. Y. Huang, G. He, Y. Yang, S. Hashimoto and R. J. Gordon, *Chem. Phys. Lett.*, **229** 621 (1994).
6. A. M. Wodtke, E. J. Hintsa, J. Somorjai and Y. T. Lee, *Isr. J. Chem.*, **29** 383 (1989).
7. G. J. Mains, L. M. Raff and S. A. Abrash, *J. Phys. Chem.*, **99** 3532 (1995).
8. M. J. Rossi and H. Helm, *J. Chem. Phys.*, **87** 902 (1987).
9. Y. Huang, Y. Yang, G. He and R. J. Gordon, *J. Chem. Phys.*, **99** 2752 (1993).
10. P. Bartolomé, M. Castillejo, J. M. Figuera and M. Martín, *J. Photochem. and Photobiol., A: Chemistry*, **54** 11 (1990).
11. M. Castillejo, M. Martín, R. de Nalda and M. Oujja, *Chem. Phys. Lett.*, **237** 367 (1995).
12. J. Luque, J. Ruiz and M. Martín, *Chem. Phys. Lett.*, **202** 179 (1993).
13. M. Castillejo, J. M. Figuera and M. Martín, *Chem. Phys. Lett.*, **117** 181 (1985).
14. J. G. Stamper and R. F. Barrow, *J. Phys. Chem.*, **65** 250 (1961).
15. J. Ruiz and M. Martín, *Comput. Chem.*, **19** 417 (1995).
16. J. A. Coxon, Private communication.
17. J. A. Coxon, *J. Mol. Spectry.*, **117** 361 (1986).
18. J. A. Coxon and P. G. Hajigeorgiou, *J. Mol. Spectry.*, **139** 84 (1990).
19. S. C. Givertz and G. G. Ballint-Kurti, *J. Chem. Soc. Faraday Trans.*, **2** 1231 (1986).
20. E. F. van Dishoeck, M. C. van Hemert, A. Dalgarno, *J. Chem. Phys.*, **77** 3693 (1977).
21. J. Tellinghuisen, *Adv. Chem. Phys.*, **60** 299 (1985).
22. J. A. Coxon, *J. Mol. Spectry.*, **133** 96 (1989).
23. J. A. Coxon and P. G. Hajigeorgiou, *J. Mol. Spectry.*, **150** 1 (1991).
24. K. P. Huber and G. Herzberg, *"Constants of Diatomic Molecules"*, Van Nostrand Reinhold, New York, 1979.
25. *"Laser, Molecules and Methods"*, ed. J. O. Hirschfelder, R. E. Wyatt and R. B. Coalson, John Wiley, New York, 1989.
26. A. A. Radzig and B. M. Smirnov, *"Reference Data on Atoms, Molecules and Ions", Springer Ser. Chem. Phys.*, Springer Verlag, 1985.
27. D. S. Ginter, M. L. Ginter and S. G. Tilford, *J. Mol. Spectry.*, **90** 152 (1981).